Adv Polym Sci (2010) 228: 39–58
DOI:10.1007/12_2010_52

Published online: 25 March 2010

Various Aspects of the Interfacial Self-Assembly of Nanoparticles

Nicole Popp, Sergej Kutuzov, and Alexander Böker

Abstract We describe the interfacial self-assembly of nanoparticles at liquid–liquid interfaces and in block copolymers. At the interface of two immiscible liquids, the particles assemble into disordered but densely packed monolayers. This self-assembly process was investigated ex situ with scanning force microscopy (SFM) and transmission electron microscopy (TEM), and laser scanning confocal microscopy (LCSM) methods. Adsorbed particles can be crosslinked at the interface to fabricate mechanically stable capsules and membranes. In addition, it was shown by pendant drop tensiometry that Janus particles consisting of gold and iron oxide show a significantly higher interfacial activity than homogeneous gold or iron oxide nanoparticles of comparable size and chemical nature. For the self-assembly of nanoparticles in block copolymer mixtures, it was shown theoretically and experimentally that these composite materials form hierarchically ordered structures. Therefore, thin films from mixtures of a cylindrical polystyrene-*block*-poly(2-vinylpyridine), with tri-*n*-octylphosphine oxide-covered CdSe nanoparticles were prepared and investigated with SFM, TEM, and grazing-incidence small angle x-ray scattering (GISAXS) after thermal annealing.

Keywords Block copolymer/nanoparticle mixtures · Interfacial assembly · Nanoparticles · Janus particles

N. Popp and S. Kutuzov
Lehrstuhl für Physikalische Chemie II, Universität Bayreuth, 95440 Bayreuth, Germany
e-mail: nicole.popp@uni-bayreuth.de; Sergey.Kutuzov@uni-bayreuth.de

A. Böker (✉)
Lehrstuhl für Makromolekulare Materialien und Oberflächen and DWI an der RWTH Aachen e.V., RWTH Aachen University, 52056 Aachen, Germany
and
Lehrstuhl für Physikalische Chemie II, Universität Bayreuth, 95440 Bayreuth, Germany
e-mail: boeker@dwi.rwth-aachen.de

Contents

Abbreviations

DFT	Density functional theory
FLIP	Fluorescence loss induced by photobleaching
FRAP	Fluorescence recovery after photobleaching
GISAXS	Grazing-incidence small-angle X-ray scattering
LbL	Layer-by-layer
O	Oil
PS	Polystyrene
PS-*b*-P2VP	Polystyrene-*block*-poly(2-vinyl-piridine)
RhB	Rhodamine B
SCFT	Self-consistent field theory
SFM	Scanning force microscopy
TEM	Transmission electron microscopy
TOPO	Tri-*n*-octylphosphine oxide
W	Water

1 Introduction

This chapter is concerned with the increasing use of liquid interfaces as templates for the self-assembly of colloidal particles [1]. In particular, besides micrometer-sized colloids, nanoscopic particles with sizes down to a few nanometers have recently been investigated. On one hand, control of the structure formation processes at the nanometer level poses a challenging problem. On the other hand, the use of nanoparticles yields ample opportunities for the fabrication of nanostructured devices (e.g., nanoporous containers or filtering devices). In addition to the use of classical oil–water (O/W) emulsion systems, like the so-called Pickering emulsions, fluid interfaces such as found in block copolymer nanostructures can be employed. Here, the nanoparticles impart specific functions to the nanostructures, such as magnetism or charge transport, as required in magnetic data storage media or polymer-based photovoltaic devices, respectively.

1.1 Pickering Emulsions

More than a century ago, Pickering [2] and Ramsden [3] investigated paraffin–water emulsions contains solid particles such as iron oxide, silicon dioxide, barium sulfate, and kaolin and discovered that these micron-sized colloids generate a resistant film at the interface between the two immiscible phases, inhibiting the coalescence of the emulsion drops. These so-called Pickering emulsions are formed by the self-assembly of colloidal particles at fluid–fluid interfaces in two-phase liquid systems (Fig. 1).

The desorption energy, which is directly related to the stability of emulsions, depends on the particle size, particle–particle interaction and, of course, particle–water and particle–oil interactions [4, 5].

Almost 80 years after Pickering's discovery, the behavior of the colloidal particles was described theoretically by Pieranski, who argued that the assembly of spherical particles at the O/W interface was determined by a decrease of the total free energy [5]. The placement of a single particle with an effective radius r, at the interface between an oil and water leads to a decrease of the initial interfacial energy E_0 to E_1 yielding an energy difference of ΔE_1:

$$E_1 - E_0 = \Delta E_1 = -\frac{\pi \cdot r^2}{\gamma_{O/W}} \cdot \left[\gamma_{O/W} - (\gamma_{P/W} - \gamma_{P/O})\right]^2 \quad (1)$$

Here, the three contributions to the interfacial energy arise from the particle–oil interface ($\gamma_{P/O}$), the particle–water interface ($\gamma_{P/W}$), and the oil–water interface ($\gamma_{O/W}$). From (1) it is evident that, for a given emulsion system (i.e., with fixed $\gamma_{P/O}$, $\gamma_{P/W}$, and $\gamma_{O/W}$), the stability of the particle assembly is determined by the square of the particle radius r. For microscopic particles the decrease in total free energy is much larger than the thermal energy (a few k_BT, where k_B is the Boltzmann constant and T is temperature) leading to an effective confinement of large colloids to the interface. Nanoscopic particles, however, are confined to the interface by an energy reduction comparable to thermal energy. Consequently, nanoparticles are

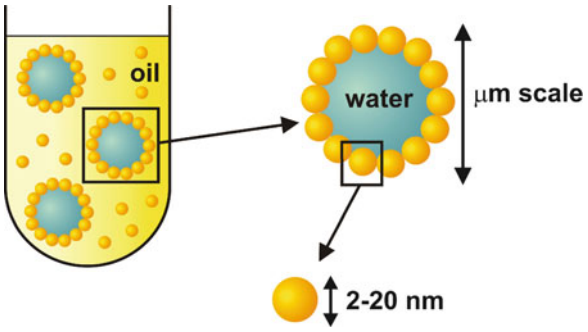

Fig. 1 Self-assembly of solid nanoparticles at the oil–water interface

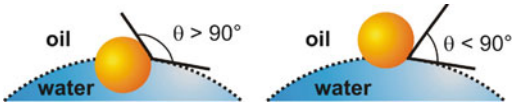

Fig. 2 Changes in wettability of solid particles at the oil–water interface at contact angles $\theta > 90°$ and $< 90°$

easily displaced from the interface, leading to a constant particle exchange at the interface, the rate of which depends on particle size. The thermally activated escape of small particles takes place more often than for larger ones and, for the equilibrium state of assembly, the total gain in free energy is lower for smaller particles. Therefore, assemblies of larger particles are more stable. This size dependence allows the nanoparticle assembly to attain their equilibrium structure at the interface, whereas micrometer-size colloids might be trapped in a non-equilibrium state. Following these theoretical thoughts, various colloidal systems with particles of different size and surface chemistry (e.g., polystyrene lattices, silica particles, etc.) were described in the literature [4, 6–9]. Moreover, the behavior of nanometer-size particles was investigated in detail due to their high potential for the construction of hierarchical and functional structures [10–13].

In addition to the size of the nanoparticles, the interfacial tension and, therefore, the wettability of a particle surface, also dictates the desorption energy [4]. The wettability is described by the contact angle θ between the solid and the oil–water interface. The stability of oil-in-water (O/W) emulsions or water-in-oil (W/O) emulsions depends on this contact angle. In general, the less-wetting liquid becomes the dispersed phase. If θ is lower than 90°, O/W emulsions are more stable; at contact angles greater than 90°, W/O emulsions are favored (Fig. 2) [14].

The variation of the desorption energy with the contact angle is displayed in Fig. 3. Binks and Lumsdon investigated a toluene–water system with constant interfacial tension of 36 mN/m by using silica nanoparticles of constant radius of 10 nm and various wettabilities [4]. At a contact angle of 90°, a maximum in desorption

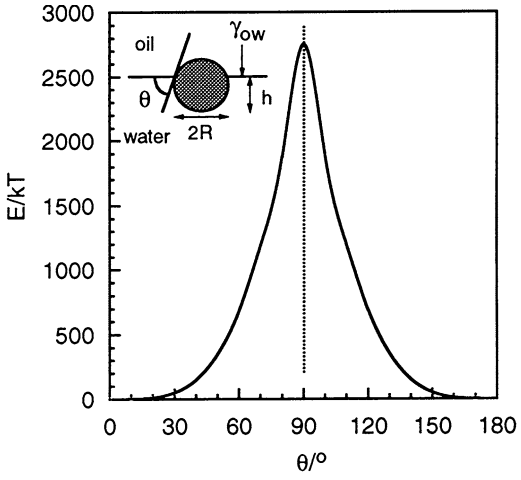

Fig. 3 Variation of the desorption energy E (equal to $k_B T$) of a spherical particle at a planar oil–water interface as a function of the contact angle θ. The depth of immersion into water is shown as h, the particle radius (R) is 10 nm, and the interfacial tension ($\gamma_{O/W}$) is 36 mN/m. Reprinted with permission from Langmuir [4]. Copyright (2000) American Chemical Society

energy was observed. Increasing or decreasing the contact angle, starting from the maximum stabilization at 90°, also decreased the stability of the emulsion. If the contact angle was between 0 and 20° or between 160 and 180°, the energy was $10\,k_BT$ or less, which is on the order of magnitude of the desorption energy of conventional surfactants [15].

So far, the stabilizing effect has only been described for particles with a homogeneous surface, i.e., a surface with homogeneous wettability. Later in this chapter, we will give a brief introduction to the theoretically anticipated behavior of particles with a heterogeneous surface exhibiting heterogeneous wettability.

1.2 Nanoparticles as Building Blocks

Besides the basic interest in the parameters governing particle interfacial assembly, there is also considerable technological potential associated with the structures formed at liquid–liquid interfaces. For example, nanoparticles could serve as building blocks for capsules and membranes with nanoscopic pores for filtering or encapsulation and for delivery purposes.

During recent years, several approaches for the design of nano- and microscopic capsules have been described in the literature. The electrostatic adsorption of polyelectrolytes [16–18] or particles [19] has also been investigated. Capsules have been successfully produced by polymerization in so-called mini-emulsions [20]. The most promising process so far uses a nanometer-to-micrometer-sized solid template of a water-insoluble substance, which is subsequently degraded to yield a hollow material [21–23]. These capsules swell in appropriate solvents and are filled by a diffusion-controlled process from the surrounding phase. The drawbacks of this method are the broad pore size distribution, and the ex situ filling procedure, during which only substances sufficiently small to pass the pores from the outside can be inserted into the capsule. Further experiments have focused on the use of liquid–liquid interfaces (i.e. water droplets dispersed in oil or a flat oil–water interface) as templates for the production of microporous capsules and membranes. Schüth, Fowler and others grew zeolite structures or silica spheres at such interfaces, but failed to generate structures with defined pore sizes and size distribution [24–28].

Pore size control in microparticle colloidal assemblies was reported by Dinsmore et al., using assembly of the particles at fluid interfaces, followed by sintering. The resulting interstices of the quasi-hexagonal array of particles gave pores in the range of several hundred nanometers [29, 30]. Furthermore, Gödel et al. fabricated elastic, nanoporous membranes from silica-polyisoprene hybrid materials spread in a Langmuir trough. Crosslinking the nanoparticle-polyisoprene film by UV radiation, followed by dissolution of the silica particles gave robust polymer membranes with pore sizes between 30 and 500 nm [31–34].

It remains a challenge, however, to fabricate capsules and membranes with precisely controlled pore size and a pore size distribution on the lower nanometer scale. Capsules with pores between 5 and 20 nm have been a long-standing goal

for encapsulation and immuno-isolation of cells for treatment of diabetes, cancer and other illnesses [35–38]. After implantation of living cells into a host, pores of this size protect the cells from the host's immune response, yet allow exchange of nutrients and secreted chemicals. Existing approaches towards fabrication of immuno-isolating capsules might result in a distribution of pore sizes too broad to be effective [35], or might require laborious lithographic processing of one capsule at a time [39].

A novel approach for the synthesis of such materials lies in the use of a nanoparticle toolkit that consists of particles with diameters ranging from 2 to 10 nm. The necessary toolkit is readily available due to the developments on nanoparticle synthesis (CdSe, Au, SiO_x, etc.) and surface functionalization methods using state-of-the-art techniques [40, 41]. So far, there are only a few publications dealing with the fluid-directed self-assembly of nanoparticles. Many papers, however, describe particle self-assembly at solid interfaces. Korgel et al. for example created self-organized superstructures from 5 nm gold particles [42–44]. Analogous experiments using CdSe, CdTe, and HgTe nanoparticles were described by Bawendi et al. [45]. First studies on the nanoparticle self-assembly at curved (droplet) interfaces in Pickering emulsions were recently published by Lin et al. [12, 46, 47], Mann et al. [48], Dai et al. [49], and Möhwald and coworkers [10, 11, 13].

1.3 Homogeneous Nanoparticles at Fluid Interfaces

The structure of CdSe nanoparticles segregated to the fluid interface as shown by confocal microscopy (Fig. 4a) has been investigated ex situ with scanning force microscopy (SFM) and transmission electron microscopy (TEM) methods. All results point to a monolayer of nanoparticles with liquidlike ordering at the interface (Fig. 4b,c) [46].

In another approach, the interfacial diffusion of the nanoparticles was determined using two photobleaching methods: fluorescence loss induced by photobleaching (FLIP) and fluorescence recovery after photobleaching (FRAP). It was found that the lateral diffusion of the nanoparticles at the interface as well as the diffusion normal to and from the interface deviated by about four orders of magnitude from the values obtained in free solution [46].

Moreover, a study using pendant drop tensiometry to follow the change in interfacial tension accompanied by simultaneous ex situ TEM measurements yielded insight into the mechanism of nanoparticle adsorption to the liquid interface [50]. As can be inferred from the data in Fig. 5, different stages of adsorption can be distinguished. The TEM images in Fig. 6 show the mechanism of nanoparticle monolayer formation in detail. First, free nanoparticle diffusion to the interface occurs. Secondly, the particles pack closer and form clusters that grow to form a closely packed particle array, lowering the interfacial tension. Finally, thermally activated exchange between adsorbed and incoming particles is observed leading to a tightly packed monolayer and only a slow decrease in interfacial tension at later times.

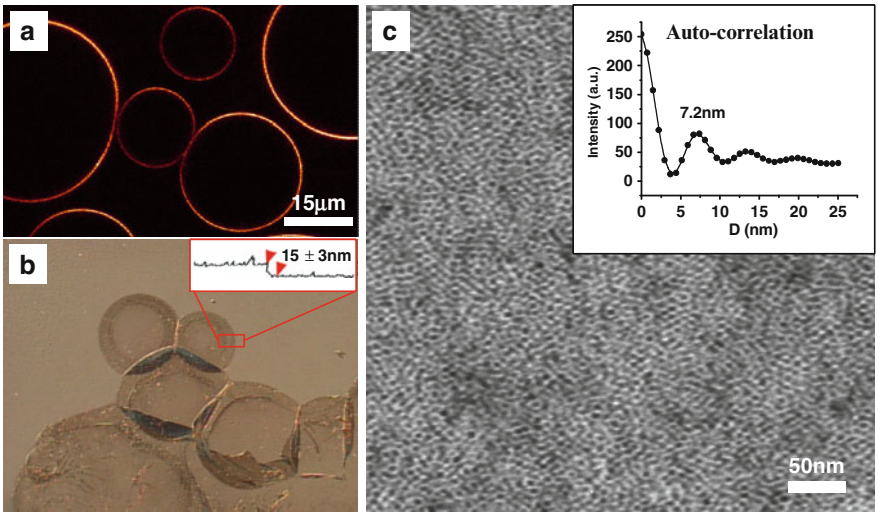

Fig. 4 (**a**) Fluorescence confocal microscope image of water droplets dispersed in toluene, covered with CdSe nanoparticles. (**b**) Differential interference contrast optical microscopy image of dried droplets on a silicon substrate. *Inset*: The atomic force microscopy height section analysis shows twice the thickness of a monolayer. (**c**) TEM image of a dried droplet. *Inset*: Auto-correlation function of the TEM image reveals a mean particle distance of 7.2 nm, which is in good agreement with the value expected for particles with 4.6 nm diameter and 0.8 nm hydrocarbon ligand. Reprinted with permission from Langmuir [46]. Copyright (2005) American Chemical Society

These observations point to the formation of a nanoparticle monolayer by nucleation and growth. Furthermore, the relationship between the free diffusion and the diffusion for the late stage of adsorption as calculated from the changes in interfacial tension reveals an energy barrier at late stages that corresponds to the activation energy for a thermally triggered escape of nanoparticles from the interface. This is in good agreement with the observed packing behavior.

To fabricate mechanically stable capsules and membranes from the spherical nanoparticle assemblies, the adsorbed particles need to be crosslinked at the interface. This can be done by the use of nanoparticles that are stabilized by reactive organic molecules. CdSe nanoparticles, stabilized by benzene vinyl ligands, segregated to the toluene–water interface and were subsequently crosslinked using a water-soluble radical initiator. This process yielded robust membranes that maintained their integrity even when removed from the interface (Fig. 7) [47]. Such crosslinked nanoparticle assemblies show high elasticity, extraordinary stability in water, and even serve as effective diffusion barriers for small molecule dyes. Using the process described above, a nanoparticle membrane has been generated in an Eppendorf tube at the toluene–water interface (Fig. 8). After removal of the organic phase and introduction of an aqueous Rhodamine B solution, a well-defined diffusion of the dye across the membrane was observed within about 15 min, without any sign of turbulent mixing (Fig. 8) [47].

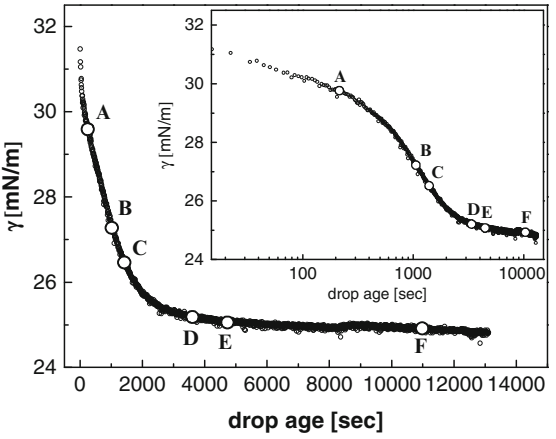

Fig. 5 Dynamic interfacial tension (γ) measurements of a toluene–water interface during adsorption of 6-nm CdSe nanoparticles to a pendant water drop in toluene (CdSe concentration was 1.58×10^{-6} mol/L). The *circles* mark the time at which TEM samples shown in Fig. 6 were prepared. The *inset* depicts the data on a logarithmic time scale. Reprinted with permission from Physical Chemistry Chemical Physics [50]. Copyright (2007) RSC Publishing

Consequently, the use of functionalized ligands attached to the nanoparticles is shown to provide an effective means of stabilizing the interfacial assembly by crosslinking. Moreover, the nanoparticle assembly proved to be as elastic and robust

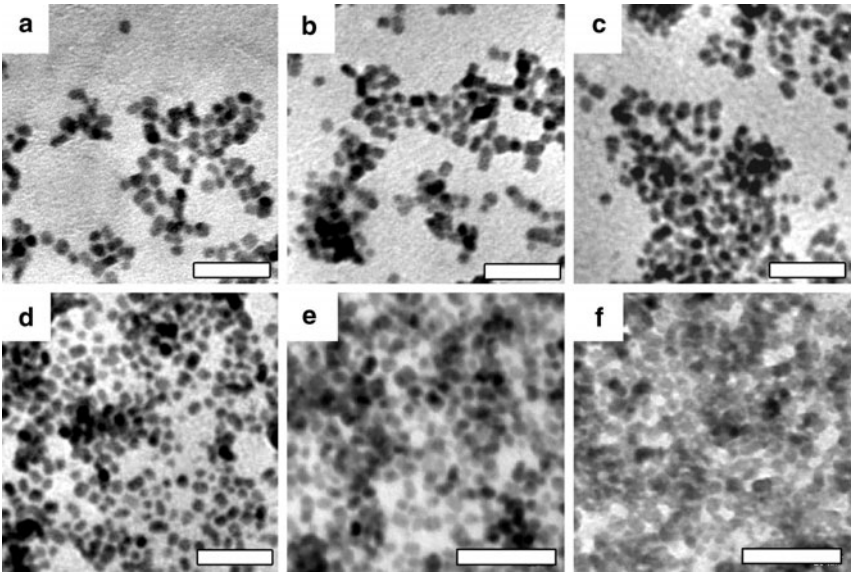

Fig. 6 Series of TEM images of 6-nm nanoparticle adsorption to the toluene–water interface at different adsorption times as marked in Fig. 5: (**a**) 230 s, (**b**) 1060 s, (**c**) 1400 s, (**d**) 3514 s, (**e**) 4700 s, and (**f**) 10,800 s. Structure formation via nucleation and growth of clusters can be seen. Scale bars: 40 nm. Reprinted with permission from Physical Chemistry Chemical Physics [50]. Copyright (2007) RSC Publishing

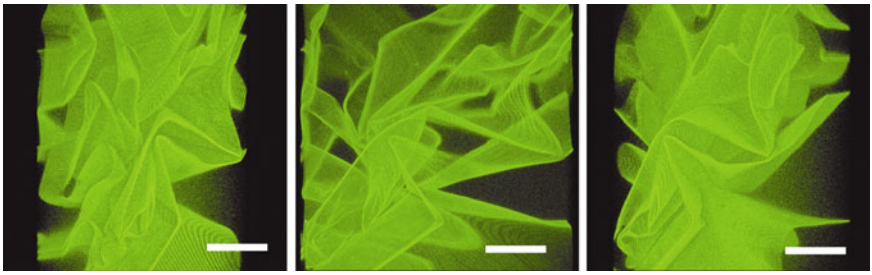

Fig. 7 Confocal microscope image from different viewing angles of a nanoparticle sheet prepared by crosslinking the functional ligands. Scale bars: 50 µm. Reprinted with permission from Journal of the American Chemical Society [47]. Copyright (2003) American Chemical Society

as expected for a nanometer thin sheet of polystyrene (PS). This work can be seen as a proof-of-concept for the use of nanoparticles as building blocks for nanoporous membranes and capsules.

A drawback of the crosslinking strategy used initially for nanoparticle assemblies is the elevated temperature (∼60°C) necessary to initiate the radical crosslinking of the vinyl benzene ligands Ligand systems have since been developed that allow crosslinking at room temperature. Ring-opening metathesis polymerization was employed using a norbornene derivative as the ligand attached to CdSe/ZnS core–shell nanoparticles in combination with a water-soluble poly(ethylene glycol)-conjugated (PEGylated) Grubbs catalyst. It was shown that these novel nanoparticles form stable assemblies at the toluene–water interface and that these assemblies could be crosslinked to yield well-defined CdSe/ZnS capsules [51]. Recently, Kotov et al. reported on the spontaneous formation of two-dimensional free-floating nanoparticle sheets from tetrahedral CdTe nanocrystals in solution [52]. Computer simulations revealed the interplay between the

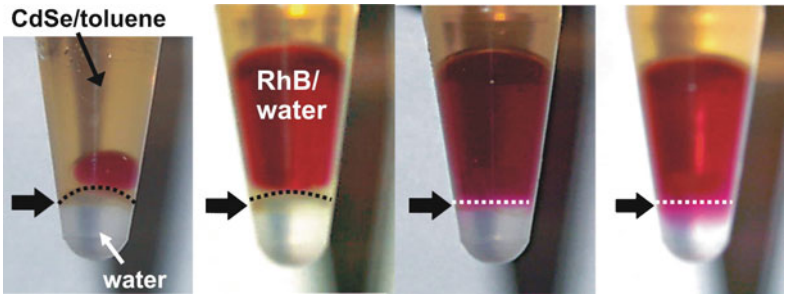

Fig. 8 Rhodamine B dye (RhB, red solution) diffusing across a membrane of crosslinked nanoparticles (*dotted line*). The *bold arrows* point to the interface in each tube. The two *right-hand* images represent a time frame of about 15 min. Subsequent addition of water to the RhB/water droplet replaces the CdSe/toluene solution leading to a RhB/water–water interface separated by the nanoparticle membrane. Reprinted with permission from Journal of the American Chemical Society [47]. Copyright (2003) American Chemical Society

electrostatic interaction and the anisotropic hydrophobic attraction between the nanoparticles to be crucial for the aggregation process. In addition, Tsukruk et al. generated free-standing polymer-nanoparticle composite films of only 20 nm thickness for sensor applications using a layer-by-layer (LbL) assembly technique [53].

1.4 Janus Particles at Fluid Interfaces

A Janus particle is defined as having two distinctly different hemispherical or surface regions; polar and apolar regions are one example. Such a particle is characterized by the contact angle of the polar region and the contact angle of the apolar region. The ratio of the areas of the polar and apolar regions can be changed, where the angle α specifies the position of the surface boundary between both regions. (Fig. 9) Values of α of either 0° or 180° correspond to homogeneous particles, while a Janus particle in the original meaning would have a value of α of 90° due to the equal polar and apolar regions [54].

As discussed by Binks and Lumsdon, amphiphilic Janus particles can exhibit an interfacial activity several times higher than simple homogeneous particles [54]. Janus particles combine the amphiphilic character of surfactants and the physical properties of nanoparticles, which opens new opportunities in emerging areas of nanotechnology and emulsion stabilization.

Recently, Perro et al. [55] reviewed the developments in the field of Janus particles over the last 15 years, describing various strategies to obtain Janus-type particles using polymer precursors. One strategy is based on the self-assembly of ABC terpolymers in bulk [56, 57] or in solution [58]. Another uses the electrostatic interactions of AB and CD diblock copolymers, which lead to inter-polyelectrolyte complexes [59]. A different synthetic concept is to obtain Janus particles made of inorganic materials, e.g., acorn-like particles made of PdS_x–Co_9S_8 [60] or

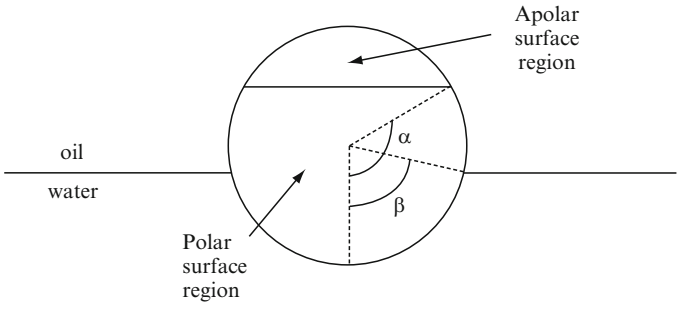

Fig. 9 Geometry of a Janus particle at the oil–water interface. The relative areas of the polar and apolar particle surface regions are parameterized by the angle α. β denotes the immersion angle of the particle at the oil–water interface. Reprinted with permission from Langmuir [54]. Copyright (2001) American Chemical Society

dumbbell-like CdS–FePt [61] and Ag–$CoFe_2O_3$ [62]. Recently, Duguet et al. showed the synthesis of an intermediate Janus particle composed of an inorganic part such as SiO_2 and an organic part consisting of PS, yielding dumbbell-like and snowman-like shapes [63]. Granick and coworkers successfully synthesized silica Janus colloid particles in large quantities at the liquid–liquid interface of molten wax and water [64, 65]. Moreover, Cohen et al. produced Janus-type microcapsules via LbL assembly followed by stamping an additional polymer layer onto one side of the LbL-capsule [62].

In addition to the efforts concerning the synthesis of Janus particles, their interfacial behavior was also of interest in order to verify Binks' predictions [54] experimentally. In this respect, it is a challenging problem – especially for polymer-based Janus structures – to clearly demonstrate the Janus character of the synthesized objects [66, 67]. The advantage of inorganic Janus particles is that they have a well-defined structure and geometry, which can often be visualized by electron microscopy. Thus, the interfacial properties of Janus particles can be directly compared to their homogeneous analogues. Recently, Glaser et al. [68] prepared Janus particles (Fig. 10) consisting of a gold part and an iron oxide part following a synthesis by Yu et al. [69]. For the Janus particles, the mean diameter of the gold particle is around 4 nm while the diameter of iron oxide is about 10 nm, resulting in an overall diameter of about 14 nm. (The diameters were determined by the image analysis program package ImageJ from the National Institutes of Health, Bethesda, MD). The homogeneous nanoparticles show a slightly smaller diameter compared to the overall size of the Janus type: the gold nanoparticle diameter is about 10 nm and the iron oxide nanoparticle diameter is about 7 nm (Fig. 10). Then, the particle amphiphilicity was tuned by ligand exchange with dodecanethiol or octadecanethiol on the gold part, and their interfacial activities were compared to those of the homogeneous gold and iron oxide particles using pendant drop tensiometry. The reduction in interfacial energy supported the theoretical predictions of Binks and Lumsdon (Fig. 11) [54, 68].

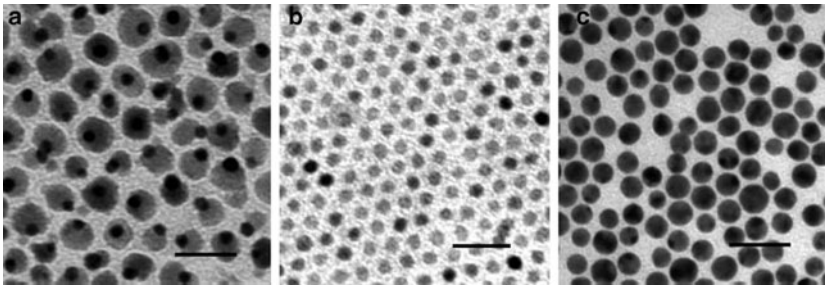

Fig. 10 TEM images of the nanoparticles: (**a**) Janus particles consisting of gold (*darker spheres*) and iron oxide (*brighter spheres*); (**b**) homogeneous iron oxide particles; (**c**) gold particles. Scale bars: 25 nm. Reprinted with permission from Langmuir [68]. Copyright (2006) American Chemical Society

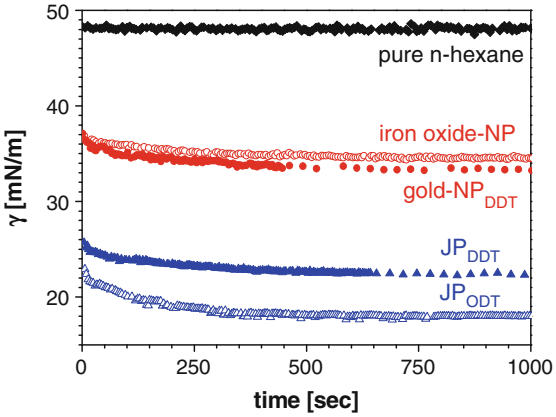

Fig. 11 Dynamic interfacial tension (γ) measurements of a hexane–water interface during adsorption of nanoparticles to a pendant water drop in hexane (for all particle types, concentration was 1.2×10^{-4} mmol/L). The gold moieties were modified using dodecanethiol (*DDT*) or octadecanethiol (*ODT*). *NP* homogeneous nanoparticles, *JP* Janus particles. Reprinted with permission from Langmuir [68]. Copyright (2006) American Chemical Society

1.5 Self-Assembly of Nanoparticle/Block Copolymer Mixtures

Incorporating nanoparticles into polymer matrices produces novel hybrid materials with special electrical, magnetic, and optical properties. One approach is to directly evaporate or synthesize inorganic nanoparticles inside well-ordered block polymer templates. Cohen [70], Sohn [71, 72], Möller [73] and coworkers have shown that polymer–nanoparticle composites can be generated by directly reducing the metal precursors inside block copolymer templates of different morphologies. Jaeger and coworkers demonstrated that by evaporating a series of metal nanoparticles on polystyrene-*block*-poly(methyl methacrylate) (PS-*b*-PMMA) templates, well-aligned metal wires could be obtained on the PS domains after thermal treatment at 180°C [74]. The disadvantages of these methods are lack of control of the size distributions of the nanoparticles, and lack of control of the position distributions of the nanoparticles inside the polymer matrices. Recently, Cheyne and Moffit demonstrated the formation of mesoscopic wires and cables via co-assembly of PS-decorated CdSe nanoparticles and a polystyrene-*block*-poly(ethylene oxide) (PS-*b*-PEO) block copolymer at the water–air interface [75]. Another approach was inspired by theoretical predictions of Balazs and coworkers [76–78], who calculated the morphology and thermodynamic behavior of copolymer–particle mixtures without requiring a priori knowledge of the equilibrium structures. The method combines a self-consistent field theory (SCFT) for the polymers with a density functional theory (DFT) for the particles. They applied this theory to diblock nanoparticle mixtures. The theory predicts ordered phases where particles and diblocks self-assemble into spatially periodic structures. They allowed the particles, by changing their solubility, to interact with both parts of the diblock copolymer

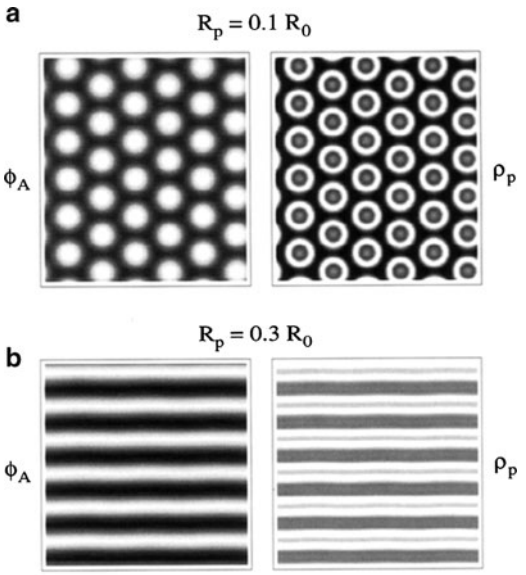

Fig. 12 Two-dimensional density plots for the diblock/particle systems obtained from the SCFT/DFT theory. Plots are for $\chi_{AB}N = 20$, $\chi_{AP} = \chi_{BP} = 0.02$, $\overline{N} = 1000$, $f = 0.35$, and $\phi_p = 0.15$. Plots on the *left* represent the distribution of the A blocks and plots on the *right* represent the distribution of the centers of mass of the particles. *Light regions* indicate a high density, while *dark regions* indicate low densities. The image in part (**a**) shows that the system displays a cylindrical phase when $R_p = 0.1R_0$ and the image in part (**b**) shows that the mixture forms a lamellar phase when the particle size is increased to $R_p = 0.3R_0$. Reprinted with permission from Macromolecules [77]. Copyright (2002) American Chemical Society

and found that variations in the particle–block interaction energies can induce phase transitions in the morphology of the mixture. At fixed interactions, variations in particle size can also induce similar transitions (Fig. 12).

Experimentally, Thomas and coworkers found that hydrocarbon-coated gold nanoparticles, with a diameter of 3.5 nm, segregated to the interface between the microdomains of poly(styrene-*block*-ethylene propylene) (PS-*b*-PEP) copolymer, whereas larger hydrocarbon-coated silica nanoparticles (21.5 nm in diameter) were located at the center of the PEP domains [79]. In the absence of specific enthalpic interactions between the two types of nanoparticles and the polymer matrix, the result suggests a profound influence of entropic contributions to the self-organization process. For large particles, the decrease in conformational entropy of the respective polymer subchains after particle sequestration is dominant, whereas for smaller particles, the decrease in entropy is outweighed by the particle translational entropy.

Manipulating the location of nanoparticles in the materials can also be achieved by controlling the surface properties of the nanoparticles. By using enthalpic interactions, Kramer and coworkers found that gold nanoparticles covered with sufficient thiol-terminated PS ligands are held inside the PS microdomains in polystyrene-*block*-poly(2-vinyl-piridine) (PS-*b*-P2VP) copolymers, whereas gold nanoparticles

covered with both PS and P2VP ligands selectively segregate to the interfaces of PS and P2VP to minimize the interfacial energies [80, 81]. A similar phenomenon was also observed by Composto and coworkers for immiscible polymer blends in the presence of silica nanoparticles [82]. Subsequent reports demonstrated that controlling the ligand density on the surface of gold nanoparticles also greatly affects the nanoparticle positional distribution inside the PS microdomains. Strong enthalpic interaction between the gold nanoparticles and pyridine units in P2VP drive the nanoparticles with low PS ligand density to the interface of PS and P2VP, whereas at high PS ligand density, the blocking of enthalpic interaction results in a distribution of gold nanoparticles inside the PS microdomains [83, 84].

In the melt, block copolymer interfaces can be considered as "fluid", with dynamics much slower than for conventional liquids. However, the use of block copolymer interfaces provides an opportunity to study the nanoparticle assembly at fluid interfaces in more detail since the polymer melt can be quenched at any stage of the assembly process. This allows the "quasi in situ" study of nanoparticle assembly at the block copolymer interfaces. Therefore, thin films from mixtures of a cylindrical PS-*b*-P2VP diblock copolymer with tri-*n*-octylphosphine oxide-(TOPO)-covered CdSe nanoparticles were prepared and investigated with SFM, TEM, and GISAXS after thermal annealing. Surprisingly, these composite materials are found to form hierarchically ordered structures via a cooperative self-organization. On the one hand, the cylindrical microdomains of the copolymer dictate the spatial distribution of the nanoparticles within the film. On the other hand, nanoparticles are found to segregate to the interfaces, mediating interfacial interactions and surface energies, resulting in an orientation of the cylindrical domains normal to the surface, even when the interactions of one of the blocks with the substrate are strongly attractive (Fig. 13). Thus, the synergy between two assembly processes produces unique structures, without the use of external fields, and opens a novel route to new self-directing, self-assembling architectures [85].

To reveal the details of the cooperative self-organization of the PS-*b*-P2VP block copolymer/nanoparticle composites leading to the above-described hierarchically

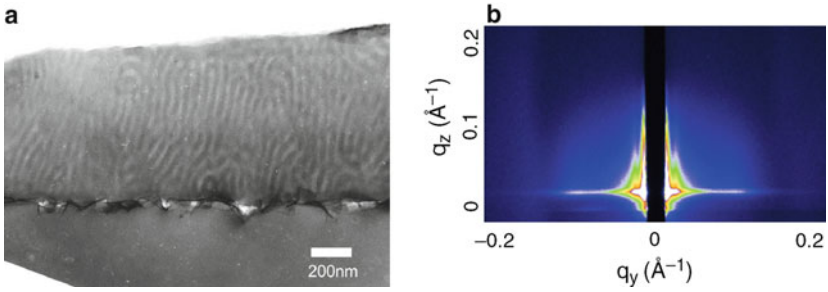

Fig. 13 (**a**) TEM image of cross-section of a PS-*b*-P2VP block copolymer/CdSe nanoparticle film after annealing at 170°C for 2 days. (**b**) Data from GISAXS measurements: of the same film at incident angle of 0.09° with a penetration depth of 61 Å. Reprinted with permission from Nature [85]. Copyright (2005) Nature Publishing Group

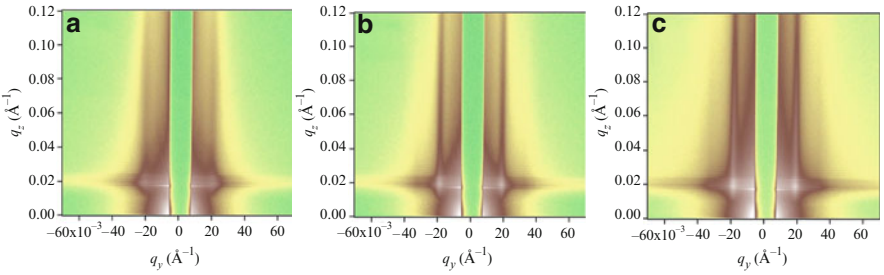

Fig. 14 Series of in-situ GISAXS images of a cylindrical nanoparticle-doped PS-*b*-P2VP film during thermal annealing at 180°C: (**a**) 0 h, (**b**) 4 h, and (**c**) 14 h after spin coating. Reprinted with permission from Advanced Materials [86]. Copyright (2007) Wiley-VCH

ordered structures, the structure formation process was investigated with in situ GISAXS during thermal annealing. It was found that the orientation of the microdomains starts at the free surface and propagates into the film (Fig. 14), while the CdSe nanoparticles segregate to the P2VP phase, filling the cylinders from the top. To demonstrate the universality of this process, lamellar microdomain morphologies were used in addition to cylindrical ones. The results are shown in the SEM image in Fig. 15, where the microdomains of a lamellar PS-*b*-P2VP block copolymer oriented perpendicular to the substrate can be seen. The inset depicts the decoration of the lamellae with CdSe nanoparticles (bright spots).

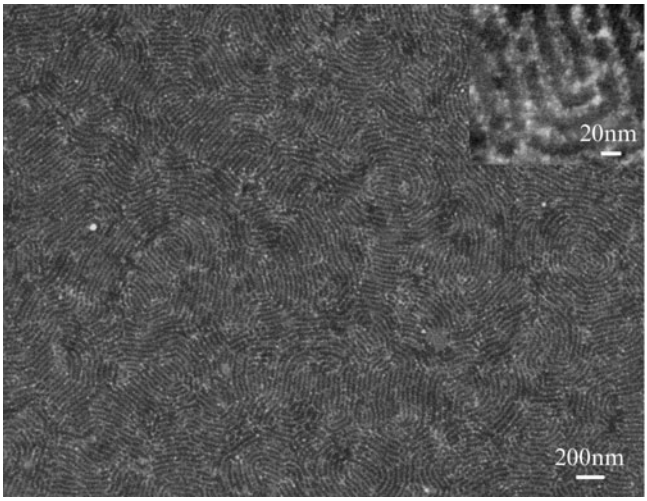

Fig. 15 High resolution SEM image of the lamellar PS-*b*-P2VP/CdSe nanoparticle composite thin film after annealing in $CHCl_3$ for 1 day, without staining. The image is taken at 1 kV acceleration voltage. Reprinted with permission from Advanced Materials [86]. Copyright (2007) Wiley-VCH

2 Conclusion

The interfacial self-assembly of nanoparticles has been discussed and examples are highlighted above. For liquid–liquid interfaces, the reduction in the interfacial energy is the dominated driving force. Nanoparticles assemble at the interface of two immiscible liquids in a disordered but densely packed monolayer. With increasing surface coverage, there exists an increasing difference between the diffusion at the early and late stages of adsorption. This reveals an energy barrier at late stages that corresponds to the activation energy for a thermally triggered escape of nanoparticles from the interface.

A promising application of the self-assembly of nanoparticles at droplet surfaces is the interfacial crosslinking of chemically functionalized nanoparticles. This enables the encapsulation of water-soluble or oil-soluble materials inside the resulting nanocontainers. By varying the concentration of reactive moieties, it will be possible to control the permeability and strength of these nanostructured membranes.

A special case of nanoparticle self-assembly is the Janus particle. It was shown that Janus particles are considerably more active than homogeneous particles of comparable size and chemical nature and that the interfacial activity can be increased by increasing the amphiphilic character of the particles. Thus, the Janus particles show a significant advantage in the stabilization of emulsions and foams over homogeneous particles as they unify the Pickering concept and the amphiphilicity of a simple surfactant.

For the self-assembly of nanoparticles in block copolymers, it was shown that these composite materials form hierarchically ordered structures via a cooperative self-organization: The microdomains of the copolymer dictate the spatial distribution of the nanoparticles within the film. The nanoparticles segregate to the interfaces, mediating interfacial interactions and surface energies, resulting in an orientation of the block copolymer domains normal to the surface. With respect to the wide range of synthetic methods for the production of well-defined nanoparticles of various types, the self-assembly of nanoparticles into hierarchically ordered structures, using interfacial interactions, represents a rich new area leading to potential applications in optical, acoustic, electronic, and magnetic materials.

Acknowledgments The authors thank C. Abetz, D.J. Adams, A. Balazs, D. Cookson, A. D. Dinsmore, T. Emrick, J. He, G. Krausch, X. Li, Y. Lin, S. Long, T.P. Russell, K. Sill, H. Skaff, R. Tangirala, J. Wang, Q. Wang, H. Xiang. This work was funded by the German Science Foundation (SFB 481, TP B10).

References

1. Binks BP (2007) Colloidal particles at liquid interfaces. Phys Chem Chem Phys 9(48):6298–6299
2. Pickering SU (1907) Emulsions. J Chem Soc 91:2001

3. Ramsden W (1903) Separation of solids in the surface-layers of solutions and 'suspensions' (observations on surface-membranes, bubbles, emulsions, and mechanical coagulation). Preliminary account. Proc R Soc Lond A Math Phys Eng Sci 72:156–164
4. Binks BP, Lumsdon SO (2000) Influence of particle wettability on the type and stability of surfactant-free emulsions. Langmuir 16(23):8622–8631
5. Pieranski P (1980) Two-dimensional interfacial colloidal crystals. Phys Rev Lett 45(7):569–572
6. Binks BP, Lumsdon SO (2001) Pickering emulsions stabilized by monodisperse latex particles: effects of particle size. Langmuir 17(15):4540–4547
7. Binks BP, Whitby CP (2004) Silica particle-stabilized emulsions of silicone oil and water: aspects of emulsification. Langmuir 20(4):1130–1137
8. Giermanska-Kahn J et al (2002) A new method to prepare monodisperse Pickering emulsions. Langmuir 18(7):2515–2518
9. Horozov TS et al (2003) Order-disorder transition in monolayers of modified monodisperse silica particles at the octane-water interface. Langmuir 19(7):2822–2829
10. Duan H et al (2005) Magnetic colloidosomes derived from nanoparticle interfacial self-assembly. Nano Lett 5(5):949–952
11. Duan HW et al (2004) Directing self-assembly of nanoparticles at water/oil interfaces. Angew Chem Int Ed 43(42):5639–5642
12. Lin Y et al (2003) Nanoparticle assembly and transport at liquid-liquid interfaces. Science 299(5604):226–229
13. Wang DY, Möhwald H (2004) Template-directed colloidal self-assembly – the route to 'top-down' nanochemical engineering. J Mater Chem 14(4):459–468
14. Schulman JH, Leja J (1954) Control of contact angles at the oil–water–solid interfaces – emulsions stabilized by solid particles (Baso4). Trans Faraday Soc 50(6):598–605
15. Aveyard R, Clint JH, Horozov TS (2003) Aspects of the stabilisation of emulsions by solid particles: effects of line tension and monolayer curvature energy. Phys Chem Chem Phys 5(11):2398–2409
16. Caruso F, Caruso RA, Möhwald H (1998) Nanoengineering of inorganic and hybrid hollow spheres by colloidal templating. Science 282(5391):1111–1114
17. Cha JN et al (2003) Spontaneous formation of nanoparticle vesicles from homopolymer polyelectrolytes. J Am Chem Soc 125:8285
18. Decher G (1997) Fuzzy nanoassemblies: toward layered polymeric multicomposites. Science 277(5330):1232–1237
19. Marinakos SM et al (1999) Gold particles as templates for the synthesis of hollow polymer capsules. Control of capsule dimensions and guest encapsulation. J Am Chem Soc 121(37):8518–8522
20. Tiarks F, Landfester K, Antonietti M (2001) Preparation of polymeric nanocapsules by miniemulsion polymerization. Langmuir 17(3):908–918
21. Caruso F et al (2000) Enzyme encapsulation in layer-by-layer engineered polymer multilayer capsules. Langmuir 16(4):1485–1488
22. Caruso F et al (2000) Microencapsulation of uncharged low molecular weight organic materials by polyelectrolyte multilayer self-assembly. Langmuir 16(23):8932–8936
23. Gao CY et al (2002) Spontaneous deposition of water-soluble substances into microcapsules: phenomenon, mechanism, and application. Angew Chem Int Ed 41(20):3789–3793
24. Fowler CE, Khushalani D, Mann S (2001) Interfacial synthesis of hollow microspheres of mesostructured silica. Chem Commun (19):2028–2029
25. Huo Q et al (1997) Preparation of hard mesoporous silica spheres. Chem Mater 9:14
26. Lu YF et al (1999) Aerosol-assisted self-assembly of mesostructured spherical nanoparticles. Nature 398(6724):223–226
27. Schacht S et al (1996) Oil-water interface templating of mesoporous macroscale structures. Science 273:768
28. Tricoli V, Sefcik J, McCormic AV (1997) Synthesis of oriented zeolite membranes at the interface between two fluid phases. Langmuir 13:4193

29. Dinsmore AD, Crocker JC, Yodh AG (1998) Self-assembly of colloidal crystals. Curr Opin Colloid Interface Sci 3(1):5–11
30. Dinsmore AD et al (2002) Colloidosomes: selectively permeable capsules composed of colloidal particles. Science 298:1006–1009
31. Mallwitz F, Goedel WA (2001) Physically cross-linked ultrathin elastomeric membranes. Angew Chem Int Ed 40(14):2645–2647
32. Xu H, Goedel WA (2002) Polymer-silica hybrid monolayers as precursors for ultrathin free-standing porous membranes. Langmuir 18(6):2363–2367
33. Xu H, Goedel WA (2003) From particle-assisted wetting to thin free-standing porous membranes. Angew Chem Int Ed 42:4694
34. Xu H, Goedel WA (2003) Particle-assisted wetting. Langmuir 19:4950
35. Chaikof EL (1999) Engineering and material considerations in islet cell transplantation. Annu Rev Biomed Eng 1:103
36. Joki T et al (2001) Continuous release of endostatin from microencapsulated engineered cells for tumor therapy. Nat Biotechnol 19:35
37. Lanza RP, Langer R, Vacanti J (2000) Principles of tissue engineering. Academic, San Diego
38. Read T-A et al (2001) Local endostatin treatment of gliomas administered by microencapsulated producer cells. Nat Biotechnol 19:29
39. Desai TA, Hansford DJ, Ferrari M (2000) Micromachined interfaces: new approaches in cell immunoisolation and biomolecular separation. Biomol Eng 17(1):23–36
40. Murray CB, Kagan CR, Bawendi MG (1995) Self-organization of Cdse nanocrystallites into 3-dimensional quantum-dot superlattices. Science 270(5240):1335–1338
41. Murray CB, Kagan CR, Bawendi (2000) Synthesis and characterization of monodisperse nanocrystals and close-packed nanocrystal assemblies. Annu Rev Mater Sci 30(1):545–610
42. Korgel BA (2004) Materials science – self-assembled nanocoils. Science 303(5662): 1308–1309
43. Shah PS et al (2003) Single-step self-organization of ordered macroporous nanocrystal thin films. Adv Mater 15(12):971–974
44. Sigman MB, Saunders AE, Korgel BA (2004) Metal nanocrystal superlattice nucleation and growth. Langmuir 20(3):978–983
45. Murray CB, Norris DJ, Bawendi MG (1993) Synthesis and characterization of nearly monodisperse Cde (E = S, Se, Te) semiconductor nanocrystallites. J Am Chem Soc 115(19):8706–8715
46. Lin Y et al (2005) Nanoparticle assembly at fluid interfaces: structure and dynamics. Langmuir 21(1):191–194
47. Lin Y et al (2003) Ultrathin cross-linked nanoparticle membranes. J Am Chem Soc 125(42):12690–12691
48. Kulak A et al (2003) Controlled assembly of nanoparticle-containing gold and silica microspheres and silica/gold nanocomposite spheroids with complex form. Chem Mater 15(2):528–535
49. Dai L, Sharma R, Wu CY (2005) Self-assembled structure of nanoparticles at a liquid-liquid interface. Langmuir 21:2641–2643
50. Kutuzov S et al (2007) On the kinetics of nanoparticle self-assembly at liquid/liquid interfaces. Phys Chem Chem Phys 9(48):6351–6358
51. Skaff H et al (2005) Crosslinked capsules of quantum dots by interfacial assembly and ligand crosslinking. Adv Mater 17(17):2082–2086
52. Tang ZY et al (2006) Self-assembly of CdTe nanocrystals into free-floating sheets. Science 314(5797):274–278
53. Jiang CY et al (2004) Freely suspended nanocomposite membranes as highly sensitive sensors. Nat Mater 3(10):721–728
54. Binks BP, Fletcher PDI (2001) Particles adsorbed at the oil-water interface: a theoretical comparison between spheres of uniform wettability and “Janus” particles. Langmuir 17(16):4708–4710
55. Perro A et al (2005) Design and synthesis of Janus micro- and nanoparticles. J Mater Chem 15(35–36):3745–3760

56. Erhardt R et al (2001) Janus micelles. Macromolecules 34(4):1069–1075
57. Erhardt R et al (2003) Amphiphilic Janus micelles with polystyrene and poly(methacrylic acid) hemispheres. J Am Chem Soc 125(11):3260–3267
58. Forster S, Antonietti M (1998) Amphiphilic block copolymers in structure-controlled nanomaterial hybrids. Adv Mater 10(3):195
59. Schrage S, Sigel R, Schlaad H (2003) Formation of amphiphilic polyion complex vesicles from mixtures of oppositely charged block ionomers. Macromolecules 36(5):1417–1420
60. Teranishi T et al (2004) Nanoacorns: anisotropically phase-segregated CoPd sulfide nanoparticles. J Am Chem Soc 126(32):9914–9915
61. Gu HW et al (2004) Facile one-pot synthesis of bifunctional heterodimers of nanoparticles: a conjugate of quantum dot and magnetic nanoparticles. J Am Chem Soc 126(18):5664–5665
62. Li ZF et al (2005) Layer-by-layer assembled Janus microcapsules. Macromolecules 38(19):7876–7879
63. Duguet E et al (2005) French Patent WO 2005/049195
64. Hong L, Jiang S, Granick S (2006) Simple method to produce Janus colloidal particles in large quantity. Langmuir 22(23):9495–9499
65. Jiang S et al (2008) Solvent-free synthesis of Janus colloidal particles. Langmuir 24(18): 10073–10077
66. Walther A, Matussek K, Muller AHE (2008) Engineering nanostructured polymer blends with controlled nanoparticle location using Janus particles. Acs Nano 2(6):1167–1178
67. Walther A, Muller AHE (2008) Janus particles. Soft Matter 4(4):663–668
68. Glaser N et al (2006) Janus particles at liquid-liquid interfaces. Langmuir 22:5227
69. Yu H et al (2005) Dumbbell-like bifunctional Au-Fe3O4 nanoparticles. Nano Lett 5(2):379–382
70. Boontongkong Y, Cohen RE (2002) Cavitated block copolymer micellar thin films: lateral arrays of open nanoreactors. Macromolecules 35(9):3647–3652
71. Sohn BH et al (2003) Directed self-assembly of two kinds of nanoparticles utilizing monolayer films of diblock copolymer micelles. J Am Chem Soc 125(21):6368–6369
72. Sohn BH, Seo BH (2001) Fabrication of the multilayered nanostructure of alternating polymers and gold nanoparticles with thin films of self-assembling diblock copolymers. Chem Mater 13(5):1752–1757
73. Spatz J et al (1998) Controlled mineralization and assembly of hydrolysis-based nanoparticles in organic solvents combining polymer micelles and microwave techniques. Adv Mater 10(6):473
74. Lopes WA, Jaeger HM (2001) Hierarchical self-assembly of metal nanostructures on diblock copolymer scaffolds. Nature 414(6865):735–738
75. Cheyne RB, Moffitt MG (2007) Controllable organization of quantum dots into mesoscale wires and cables via interfacial block copolymer self-assembly. Macromolecules 40(6): 2046–2057
76. Lee JY, Shou ZY, Balazs AC (2003) Predicting the morphologies of confined copolymer/nanoparticle mixtures. Macromolecules 36(20):7730–7739
77. Lee JY et al (2002) Effect of nanoscopic particles on the mesophase structure of diblock copolymers. Macromolecules 35(13):4855–4858
78. Thompson RB et al (2001) Predicting the mesophases of copolymer-nanoparticle composites. Science 292(5526):2469–2472
79. Bockstaller MR et al (2003) Size-selective organization of enthalpic compatibilized nanocrystals in ternary block copolymer/particle mixtures. J Am Chem Soc 125(18):5276–5277
80. Chiu JJ et al (2005) Control of nanoparticle location in block copolymers. J Am Chem Soc 127(14):5036–5037
81. Kim BJ et al (2005) Nanoparticle-induced phase transitions in diblock-copolymer films. Adv Mater 17(21):2618
82. Chung H et al (2005) Self-regulated structures in nanocomposites by directed nanoparticle assembly. Nano Lett 5(10):1878–1882
83. Kim BJ et al (2006) Effect of areal chain density on the location of polymer-modified gold nanoparticles in a block copolymer template. Macromolecules 39(12):4108–4114

84. Kim BJ et al (2007) Importance of end-group structure in controlling the interfacial activity of polymer-coated nanoparticles. Macromolecules 40(6):1796–1798
85. Lin Y et al (2005) Self-directed self-assembly of nanoparticle/copolymer mixtures. Nature 434(7029):55–59
86. He J et al (2007) Self-assembly of nanoparticle-copolymer mixtures: a kinetic point of view. Adv Mater 19:381–385

http://www.springer.com/978-3-642-12911-7

Complex Macromolecular Systems II
Müller, A.H.E.; Schmidt, H.-W. (Eds.)
2010, XII, 220 p. 157 illus., Hardcover
ISBN: 978-3-642-12911-7